

SUPPORTING INFORMATION

Optical Excitations and Field Enhancement in Short Graphene Nanoribbons

Caterina Cocchi,^{*,†,‡} Deborah Prezzi,^{*,†} Alice Ruini,^{†,‡} Enrico Benassi,[†] Marilia J. Caldas,[¶] Stefano Corni,[†] and Elisa Molinari^{†,‡}

Centro S3, CNR-Istituto Nanoscienze, I-41125 Modena, Italy, Dipartimento di Fisica, Università di Modena e Reggio Emilia, I-41125 Modena, Italy, and Instituto de Física, Universidade de São Paulo, 05508-900 São Paulo, SP, Brazil

E-mail: caterina.cocchi@unimore.it; deborah.prezzi@unimore.it

^{*}To whom correspondence should be addressed

[†]Centro S3, CNR-Istituto Nanoscienze, I-41125 Modena, Italy

[‡]Dipartimento di Fisica, Università di Modena e Reggio Emilia, I-41125 Modena, Italy

[¶]Instituto de Física, Universidade de São Paulo, 05508-900 São Paulo, SP, Brazil

Excitation Analysis in Terms of Orbital Transitions and Weights

In Table S1 we report the lowest energy excitations, labeled after Figure 1(b) in the main text, of three graphene nanoflakes (GNFs) at increasing length. We consider the shortest ($N_L=10$, ~ 24 Å) and the longest ($N_L=40$, ~ 88 Å) ones, in addition to $N_L=28$ GNF (length ~ 63 Å) discussed in details in the main text. The excitation energy, oscillator strength (OS) and composition in terms of molecular orbital (MO) transitions for the main excitations are presented.

From the results presented in Table S1, the gain of OS characterizing the first bright excitation L1 at increasing length is evident. It is also worth noting that for the longest considered ribbon ($N_L=40$) the lowest energy excitation is indeed L1, being basically degenerate with T1.

System	Excitation	Energy [eV]	OS	Transitions (weight)
$N_L=10$	T1	2.54	0.0005	HOMO-1 \rightarrow LUMO (0.37) HOMO \rightarrow LUMO+1 (0.39)
	L1	2.72	1.62	HOMO \rightarrow LUMO (0.79)
	L2	3.32	5.43	HOMO-3 \rightarrow LUMO+3 (0.12) HOMO-1 \rightarrow LUMO+1 (0.76)
	LW	3.48	0.34	HOMO-4 \rightarrow LUMO (0.14) HOMO-2 \rightarrow LUMO+2 (0.26) HOMO \rightarrow LUMO+4 (0.31)
	T2	3.59	1.56	HOMO-1 \rightarrow LUMO (0.41) HOMO \rightarrow LUMO+1 (0.39)

Continued on next page

Table S1 – continued from previous page

System	Excitation	Energy [eV]	OS	Transitions (weight)
$N_L=14$	T1	2.48	0.00	HOMO-3 \rightarrow LUMO (0.21) HOMO \rightarrow LUMO+3 (0.22)
	L1	2.51	8.19	HOMO-2 \rightarrow LUMO+2 (0.11) HOMO-1 \rightarrow LUMO+1 (0.21) HOMO \rightarrow LUMO (0.48)
	LW	2.78	0.35	HOMO-2 \rightarrow LUMO (0.21) HOMO-1 \rightarrow LUMO+1 (0.15) HOMO \rightarrow LUMO+2 (0.23)
	L2	3.07	10.00	HOMO-6 \rightarrow LUMO+6 (0.12) HOMO-4 \rightarrow LUMO+4 (0.20) HOMO-3 \rightarrow LUMO+3 (0.48)
	T2	3.57	3.35	HOMO-4 \rightarrow LUMO+2 (0.16) HOMO-3 \rightarrow LUMO (0.18) HOMO-1 \rightarrow LUMO+4 (0.15) HOMO \rightarrow LUMO+3 (0.17)

Continued on next page

Table S1 – continued from previous page

System	Excitation	Energy [eV]	OS	Transitions (weight)
$N_L=40$	L1	2.48	12.56	HOMO-2 \rightarrow LUMO+2 (0.13)
				HOMO-1 \rightarrow LUMO+1 (0.19)
				HOMO \rightarrow LUMO (0.36)
	T1	2.48	0.00	HOMO-4 \rightarrow LUMO (0.15)
				HOMO \rightarrow LUMO+4 (0.16)
	LW	2.68	0.62	HOMO-2 \rightarrow LUMO (0.18)
				HOMO-1 \rightarrow LUMO+1 (0.11)
				HOMO \rightarrow LUMO+3 (0.19)
	L2	3.03	13.30	HOMO-7 \rightarrow LUMO+7 (0.12)
				HOMO-5 \rightarrow LUMO+5 (0.19)
				HOMO-4 \rightarrow LUMO+4 (0.35)
	T2	3.59	5.16	HOMO-4 \rightarrow LUMO (0.14)
				HOMO \rightarrow LUMO+4 (0.13)

Table S1: Energy, oscillator strength (OS) and composition of the main excitations characterizing the spectra of $N_W=7$ GNFs of length $N_L=10$, $N_L=28$ and $N_L=40$. In the last column we include the MO transitions with relative weights larger than 0.1.

In Table S2 we report the lowest energy excitations of $N_W=6$, $N_W=7$ and $N_W=8$ graphene flakes of length $N_L=28$. Excitation L1 in the largest flake ($N_W=8$) presents an increased OS of about 10% with respect to $N_W=6$ and $N_W=7$ GNF, where it keeps almost the same intensity. Also the energy of L1 is red shifted of over 1 eV in $N_W=8$ GNF, with respect to that of the other two, as observed in the UV-vis spectra of Figure 5(a) of the main text.

Table S2: Energy, oscillator strength (OS) and composition of the two lowest energy excitations of graphene nanoflakes with $N_L=28$ and different width, namely $N_W=6$, $N_W=7$ and $N_W=8$. In the last column only we include the MO transitions with relative weights larger than 0.1.

System	Excitation	Energy [eV]	OS	Transitions (weight)
$N_W=6$	L1	2.47	8.23	HOMO-1 \rightarrow LUMO+1 (0.20) HOMO \rightarrow LUMO (0.54)
$N_W=7$	T1	2.48	0.002	HOMO-3 \rightarrow LUMO (0.21) HOMO \rightarrow LUMO+3 (0.22)
	L1	2.51	8.19	HOMO-2 \rightarrow LUMO+2 (0.11) HOMO-1 \rightarrow LUMO+1 (0.21) HOMO \rightarrow LUMO (0.48)
$N_W=8$	L1	1.37	9.15	HOMO-1 \rightarrow LUMO+1 (0.18) HOMO \rightarrow LUMO (0.69)

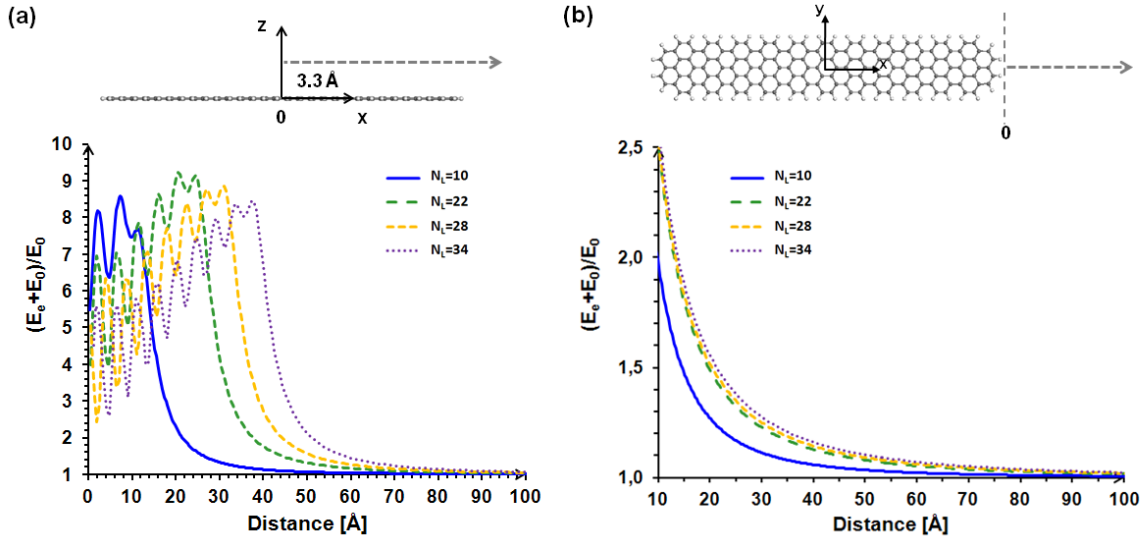


Figure S1: Field enhancement of longitudinally polarized excitation L1 for selected graphene nanoflakes of fixed width $N_W=7$ and increasing length from about 24 ($N_L=10$) to about 75 Å ($N_L=34$), computed along the flake axis (a) at 3.3 Å from its plane and (b) along the ribbon plane, starting from its lateral end. Notice that the values of the field enhancement are sensitive to the choice of Γ_p , according to Eq. (2) in the main text: here a conservative value $\Gamma_p=25$ meV is adopted.

Effects of Length Increase on the Field Enhancement

We report in Figure S1 the field enhancement produced by L1 excitation along the longitudinal (x) axis of selected graphene flakes of increasing length, at different heights from the basal plane: at 3.3 Å above the plane from the flake center [see Figure S1(a)] and along the plane from the flake end [see Figure S1(b)]. It is worth noting that above the ribbon plane the field enhancement is basically independent of the length, and the curves are characterized by an oscillating behavior related to the transition density modulation. On the other hand, further from the flake lateral border, where the dipolar character of the transition density becomes predominant [see also Figure 2(a) in the main text], the field enhancement curves follow the oscillator strength gain of L1 upon increasing length [see Table S1 and also Figure 1(c) in the main text].

Enhanced Response Field from Transition Density

We derive the relation between the enhanced field and the transition properties of the molecule. In general, the electric field \vec{E}_e produced by the polarization of the molecule due to an external potential V_0 oscillating at a frequency ω (for example, due to an external electric field \vec{E}_0 considered in the quasi-static limit) can be found from:

$$\nabla \cdot \vec{E}_e = 4\pi\delta\rho(\vec{r}) \quad (1)$$

where $\delta\rho(\vec{r})$ is the electronic density induced in the position \vec{r} by \vec{E}_0 . From response theory, it comes:¹

$$\delta\rho(\omega; \vec{r}) = \int \chi(\omega; \vec{r}, \vec{r}') V_0(\vec{r}') d\vec{r}', \quad (2)$$

where the molecular response function can be written as:

$$\chi(\omega; \vec{r}, \vec{r}') = \sum_{i \neq 0} \frac{\rho_{0i}(\vec{r})\rho_{i0}(\vec{r}')}{\hbar\omega + i\hbar\Gamma_i + E_i - E_0} + \frac{\rho_{i0}(\vec{r})\rho_{0i}(\vec{r}')}{-\hbar\omega - i\hbar\Gamma_i + E_i - E_0} \quad (3)$$

In Eq. (3), ρ_{0i} are the transition densities between the ground state 0 and the excited state i , and E_i are the energies of the states. When the frequency ω is close to a molecular transition from 0 to p (i.e., $\omega \approx \omega_{p0} = (E_p - E_0)/\hbar$), one denominator in Eq. (3) becomes very small, and the corresponding term dominates the sum over i , so that:

$$\chi(\omega_{p0}; \vec{r}, \vec{r}') \approx \frac{\rho_{0p}(\vec{r})\rho_{p0}(\vec{r}')}{i\hbar\Gamma_p}. \quad (4)$$

Therefore:

$$\delta\rho(\omega; \vec{r}) = \frac{\rho_{0p}(\vec{r})}{i\hbar\Gamma_p} \int \rho_{p0}(\vec{r}') V_0(\vec{r}') d\vec{r}'. \quad (5)$$

If we now assume that $V_0(\vec{r}')$ is the electrostatic potential associated with an external probing field in the quasi static limit, then:

$$V_0(\vec{r}') = -\vec{r}' \cdot \vec{E}_0 \quad (6)$$

and

$$\delta\rho(\omega_{p0}; \vec{r}) = -\frac{\rho_{0p}(\vec{r})}{i\hbar\Gamma_p} \vec{\mu}_{p0} \cdot \vec{E}_0, \quad (7)$$

where $\vec{\mu}_{p0}$ is the molecular transition dipole, evaluated here by the ZINDO/S method. By solving Eq. (1) using the expression of $\delta\rho(\omega; \vec{r})$ in Eq. (7), the electric potential and the field \vec{E}_e plotted in Figure 3 and Figure 4 of the main text are finally obtained.

References

- (1) Fetter, A. L.; Walecka, J. D. *Quantum theory of many-particle systems*; McGraw-Hill, New York, 1971.